A model for preferential concentration

H. Sigurgeirsson and A. M. Stuart

Citation: Phys. Fluids **14**, 4352 (2002); doi: 10.1063/1.1517603
View online: http://dx.doi.org/10.1063/1.1517603
View Table of Contents: http://pof.aip.org/resource/1/PHFLE6/v14/i12
Published by the AIP Publishing LLC.

A model for preferential concentration

H. Sigurgeirsson[a)]
SCCM Program, Stanford University, Stanford, California 94305

A. M. Stuart
Mathematics Institute, Warwick University, Coventry, CV4 7AL, England

(Received 8 May 2002; accepted 9 September 2002; published 6 November 2002)

The preferential concentration of inertial particles in a turbulent velocity field occurs when the particle and fluid time constants are commensurate. We propose a straightforward mathematical model for this phenomenon and use the model to study various scaling limits of interest and to study numerically the effect of interparticle collisions. The model comprises Stokes' law for the particle motions, and a Gaussian random field for the velocity. The primary advantages of the model are its amenability to mathematical analysis in various interesting scaling limits and the speed at which numerical simulations can be performed. The scaling limits corroborate experimental evidence about the lack of preferential concentration for a large and small Stokes number and make new predictions about the possibility of preferential concentration at large times and lead to stochastic differential equations governing this phenomenon. The effect of collisions is found to be negligible for the most part, although in some cases they have an interesting antidiffusive effect. © *2002 American Institute of Physics.* [DOI: 10.1063/1.1517603]

I. INTRODUCTION

Empirical evidence indicates that, in some parameter regimes, the distribution of particles in a turbulent velocity field is highly correlated with the turbulent motions, a phenomenon that has been termed *preferential concentration*.[1] The basic physics underlying this phenomenon is the fact that inertial particles spin out from the center of eddies; if the particle and fluid time constants are commensurate, so that the eddy persists on this spinout time scale, then the particles will concentrate in regions where straining dominates vorticity.[1,2]

Our aims in this work are the following: (i) to describe a simple model for preferential concentration; (ii) to use the model to elucidate a number of interesting scaling limits; (iii) to study preferential concentration through a numerical simulation of the model; and (iv) to study whether collisions between particles become important in view of the high particle densities present, where preferential concentration occurs.

We study two-dimensional problems, using Stokes' law to describe particle motions, and modeling the velocity as a Gaussian random field that is incompressible, homogeneous, isotropic, periodic in space, stationary and Markovian in time. The resulting model is both cheap to simulate and amenable to analysis in various important scaling limits. These two facts give the model its primary advantage over models that employ direct numerical simulation (DNS), or large eddy simulation, for the velocity field.

To illustrate the physical phenomena of interest, we describe some experimental data. Figure 1 is taken from Fessler *et al.*[3] It shows the distribution of particles in a turbulent fluid at a Stokes number (the ratio of the particle to fluid time constants) of order 1. Figure 2, also taken from Fessler *et al.*,[3] is a quantitative representation of the information in Fig. 1. It is obtained by overlaying a square grid on Fig. 1, then counting the number of particles inside each square of the grid and making a histogram of the resulting collection of numbers. The comparison is with a Poisson distribution, which is what would be observed if the particles were placed independently at random, with a mean number of particles in a volume element being proportional to volume. The comparison quantifies the observation that, in Fig. 1, there are substantial areas where particle density is very low, and where it is very high. Experiments at high or low Stokes number do not exhibit this phenomenon.

In Sec. II we introduce the mathematical model, and highlight the main parameters: shape of the energy spectrum, time scale ratio, eddy correlation time, and eddy correlation length; we also discuss the limitations of the model. In Sec. III we describe various scaling limits in which the model simplifies, using the methodology described in Majda *et al.*[4] and Kramer and Majda.[5] Section IV contains the results of numerical simulations for varying Stokes number, showing agreement with experimental evidence such as that in Fig. 2. The effects of elastic collisions are also studied in this section. In Sec. V we show various simulations of the large time scaling limits derived in Sec. III.

There is an extensive literature describing experiments on inertial particles in turbulent flows; see Eaton and Fessler[1] for a review of the subject, and for further references. There has also been work studying inertial particles in turbulent flows, using DNS of the Navier–Stokes equations; relevant references include Squires and Eaton,[2,6,7] which describe numerically generated data on particle distributions, and their relation to experimental data and to invariants of the fluid velocity field, and Hogan *et al.*[8] and Elperin *et al.*,[9,10] who study the finer properties of the particle distributions such as self-similarity; Crisanti *et al.*[11] is also of interest in this con-

[a)]Present address: deCODE Genetics, 101 Reykjavik, Iceland.

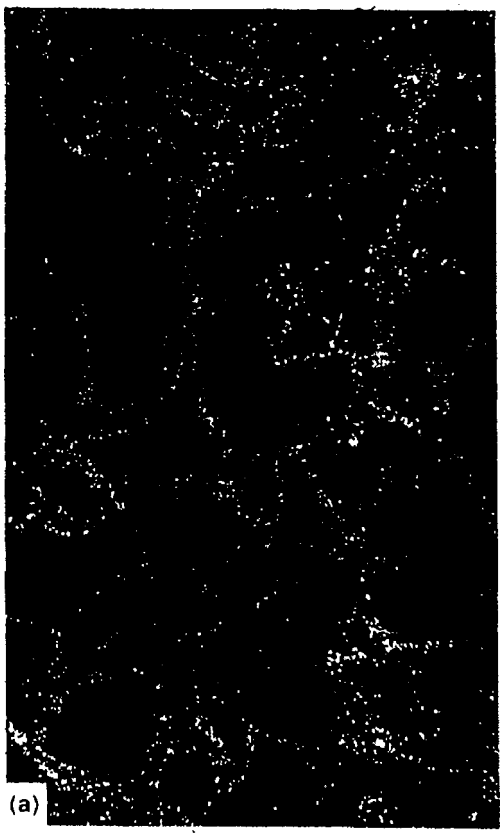

FIG. 1. Photograph of 28 μm lycopodium particles illuminated by a laser sheet on the center plane of a vertical turbulent channel flow. Reproduced, with permission, from Ref. 3.

text, although the model for particle motion differs slightly from that used here and in the other references. Sundaram and Collins[12] study the effect of collisions using DNS of the Navier–Stokes equations. There is also work, motivated by planet formation, for example, on particle aggregation in rotating flows.[13] The mechanism in this case is related to, but distinct from, that which we study here.

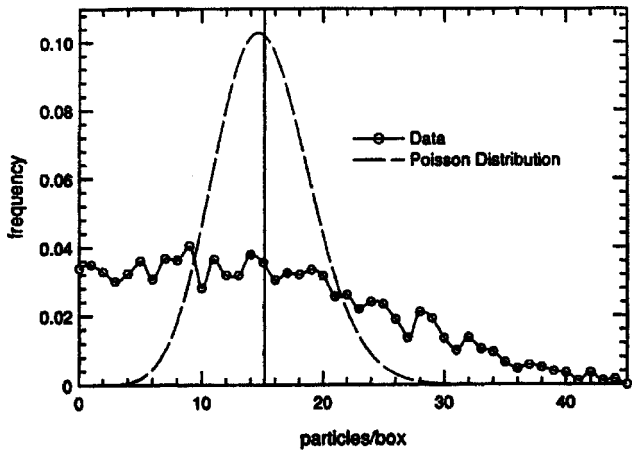

FIG. 2. The distribution of particle number density for 28 μm lycopodium particles, St$=0.7$ on a 2 mm square grid. Also plotted is Poisson, or random distribution, for the same mean number of particles per box. Reproduced, with permission, from Ref. 3.

Concerning literature on inertial particles in synthetic turbulence, that is, a random velocity field model chosen to match some of the statistics of turbulence, there are few references; see Maxey[14] for work in this direction. However, there is considerable literature on random velocity fields as models of turbulence in the noninertial context; the seminal paper by Kraichnan[15] indicated the viability of this approach and the more recent papers of Careta *et al.*,[16] Martí *et al.*,[17] and Juneja *et al.*[18] employ the particular periodic implementation of Kraichnan's idea that we use here. In particular, the papers Careta *et al.*,[16] and Martí *et al.*,[17] and the book by García-Ojalvo and Sancho (Ref. 19, pp. 108–113), describe the PDE formulation of synthetic turbulent velocity fields that we use, together with advocating the use of the Fourier transform to simulate such velocity fields efficiently on a computer, an approach that we follow.

Also of interest are studies of fluid particles, or passive tracers, in synthetic turbulence,

$$\dot{x}(t)=v(x(t),t), \tag{1}$$

since they are closely related to our model (7) in the limit of zero time scale ratio ($\tau\to 0$). This work dates back to an early model of Taylor[20] with a recent study of this problem being described in, for example, Fannjiang and Komorowski[21] and Komorowski and Papanicolaou.[22] The papers by Carmona and Xu,[23] Carmona *et al.*[24] and Fannjiang and Komorowski[21] employ, and study the properties of, the formulation of the Gaussian random field through use of an Ornstein–Uhlenbeck process, as we do here. The review article by Majda and Kramer[25] gives an extensive background on the subject of passive tracers in turbulent fluid and, in particular, overviews the subject of how to create random fields that model certain characteristics of turbulent fluids.

In this paper we are interested in N-point motions in a random field: the study of correlations among N particles moving in a (model for a) turbulent fluid; in particular, we are interested in the case of $N\gg 1$ so that we can study particle distributions in a meaningful way. Mathematically speaking, we are studying a stochastic flow,[26] and in this field the study of two-point motions plays a central role. There is some literature on the topic of two-point motion in the context of particle tracers.[27,28]

In conclusion we show the following: (i) that a simple Gaussian random field model for the velocity field, coupled with Stokes' law for particle motion, provides remarkably good agreement with some of the experimental data concerning preferential concentration; (ii) the model allows for an elucidation of various scaling limits that either confirm experimental observation (for small or large Stokes number) or provide new insight into large time behavior, predicting preferential concentration in some cases, and giving stochastic differential equations governing the phenomenon; (iii) the model is fast to simulate, giving an order of magnitude speedup over DNS simulations; (iv) the effect of collisions can be studied numerically, using the fast algorithm in Sigurgeirsson *et al.*,[29] and our results show that the effect of collisions is negligible here; to the extent that they are no-

ticeable they create an interesting antidiffusive behavior, sharpening concentration lines in the particle distributions.

II. MATHEMATICAL MODEL

We consider the motion of a particle in two dimensions with position $x(t)$ at time t, moving in a fluid according to Stokes' law:

$$\tau\ddot{x}(t)=v(x(t),t)-\dot{x}(t). \tag{2}$$

Here $\tau=m/(\mu C)$ where m is the particle mass, μ is the fluid viscosity, C is a universal nondimensional constant, and $v(x,t)$ is the prescribed velocity field of the fluid. We neglect the finite-end effect corrections to C that make the law nonlinear, through a logarithmic dependence on particle Reynolds number[30] in two dimensions. Furthermore, by assuming that the force on the particle is linear in the difference between particle and fluid velocity, we are making an approximation whose validity may break down at large velocity differences.[31]

Under our assumption that the velocity is two-dimensional (2-D) and incompressible, we may introduce a streamfunction ψ, so that

$$v=\nabla^{\perp}\psi:=\left(\frac{\partial\psi}{\partial x_2},-\frac{\partial\psi}{\partial x_1}\right).$$

Our assumptions that the velocity field is Gaussian, Markovian, and homogeneous are satisfied by assuming that ψ is the solution to the partial differential equation,

$$\frac{\partial\psi}{\partial t}(x,t)=\nu\Delta\psi(x,t)+\sqrt{\xi}\frac{\partial W}{\partial t}(x,t), \tag{3}$$

$$x\in\mathcal{O}\subset\mathbb{R}^2,\quad t\geqslant 0, \tag{4}$$

where $\partial W/\partial t$ is a Gaussian process, white in time. We will take $\mathcal{O}$ to be the square of side length L in two dimensions, namely $[0,L]^2$, and extend to the whole of the plane ($\mathbb{R}^2$) by periodicity. Then W has the expansion

$$W(x,t)=\sum_{k\in K}\sqrt{\lambda_k}e_k\left(\frac{x}{L}\right)\beta_k(t). \tag{5}$$

Here $K=2\pi\mathbb{Z}^2\backslash\{(0,0)\}$, $e_k(x)=e^{ik\cdot x}$, and $\{\beta_k\}_{k\in K}$ is a sequence of standard complex-valued Brownian motions, independent except $\beta_{-k}=\beta_k^*$. The *spectrum* $\{\lambda_k\}_{k\in K}$ is normalized so that

$$\sum_{k\in K}\lambda_k=1. \tag{6}$$

The parameters λ_k will be chosen so that the velocity field reproduces the desired energy spectra. However, it is important to realize that such linear Gaussian models for the velocity field do not capture important effects present in real turbulent fluids such as the energy cascade between scales, and non-Gaussian tails at fixed scales.

We introduce nondimensional variables. To that end set $t=Tt'$, $x(t)=Lx'(t')$, $\psi(x,t)=(L^2/T)\psi'(x',t')$, and $v(x,t)=(L/T)v'(x',t')$. Then $v'=\nabla^{\perp}_{x'}\psi'$ and Eqs. (2), (3), and (5) become

$$\frac{\tau}{T}\frac{d^2x'}{dt'^2}(t')=v'(x'(t'),t')-\frac{dx'}{dt'}(t'),$$

$$\frac{\partial\psi'}{\partial t'}=\frac{\nu T}{L^2}\Delta_{x'}\psi'+\frac{T\sqrt{T}}{L^2}\sqrt{\xi}\frac{\partial W'}{\partial t'},$$

$$W'(t',x')=\sum_{k\in K}\sqrt{\lambda_k}e_k(x')\beta_k'(t').$$

Here we set $\beta_k(t)=\sqrt{T}\beta_k'(t')$ so that $\{\beta_k'\}_{k\in K}$ are also standard Brownian motions. By choosing the length scale L, the problem is posed on the unit torus, $\mathbb{T}^2$, and we choose the time scale T such that $T\sqrt{\xi}=L\sqrt{\nu}$. We show below that this choice ensures that the mean square velocity is constant at every point in space and time; hence, T is a natural fluid time constant. Defining $\tau'=\tau/T$ and $\nu'=\nu T/L^2$ and dropping the primes gives

$$\begin{aligned}&\tau\ddot{x}(t)=v(x(t),t)-\dot{x}(t),\\&v=\nabla^{\perp}\psi,\\&\frac{\partial\psi}{\partial t}=\nu\Delta\psi+\sqrt{\nu}\frac{\partial W}{\partial t},\\&W(x,t)=\sum_{k\in K}\sqrt{\lambda_k}e_k(x)\beta_k(t).\end{aligned} \tag{7}$$

Henceforth we work in these dimensionless variables. The equations are augmented with periodic boundary conditions in $x\in\mathbb{T}^2$ and initial data (x_0,y_0,ψ_0) for (x,y,ψ). The initial data for ψ are chosen so that it is stationary and we show how to do this below. Doing so ensures that v itself is stationary.

The stochastic process ψ is an infinite-dimensional Ornstein–Uhlenbeck (OU) process. To get an idea of the solution, we use a separation of variables,

$$\psi(x,t)=\sum_{k\in K}\hat{\psi}_k(t)e_k(x), \tag{8}$$

for $\hat{\psi}_k:\mathbb{R}\to\mathbb{C}$, $k\in K$. Then we use the Fourier representation (7) of W giving

$$d\hat{\psi}_k=-\alpha_k\nu\hat{\psi}_k dt+\sqrt{\nu\lambda_k}d\beta_k,\quad \hat{\psi}_k(0)=\hat{\psi}_k^0, \tag{9}$$

where $\hat{\psi}_k^0:=\langle\psi_0,e_k\rangle$ and $\Delta e_k=-\alpha_k e_k$. The unique solution of this stochastic differential equation is the OU process,

$$\hat{\psi}_k(t)=e^{-\nu\alpha_k t}\hat{\psi}_k^0+\sqrt{\nu\lambda_k}\int_0^t e^{-\nu\alpha_k(t-s)}d\beta_k(s).$$

The stationary distribution of this SDE is a Gaussian $\mathcal{N}(0,\lambda_k/2\alpha_k)$. If we choose initial data from this distribution then ψ is stationary in each of its Fourier components and

$$\mathbb{E}|v(x,t)|^2=\frac{1}{2}\sum_{k\in K}\lambda_k=\frac{1}{2}.$$

To see this, note that

$$v(x,t)=\sum_{k\in K}\hat{\psi}_k(t)\nabla^{\perp}e_k(x). \tag{10}$$

As v is real, we have $\hat{v}_{-k}=\hat{v}_k^*$. For $k\in K$ the energy $\mathcal{E}(t)$ of Fourier mode k is given by (using stationarity) $\mathcal{E}_k(t)=\mathbb{E}|\hat{v}_k(0)|^2$. In the stationary distribution we have $\mathbb{E}|\hat{\psi}_k|^2=\lambda_k/2\alpha_k$ and $\mathbb{E}|\hat{v}_k|^2=|k|^2\mathbb{E}|\hat{\psi}_k|^2=|k|^2\lambda_k/2\alpha_k$. As $\alpha_k=|k|^2$ this implies that, to achieve a given mean kinetic energy spectrum $\{\mathcal{E}_k\}_{k\in K}$, we set

$$\lambda_k=2\mathcal{E}_k. \tag{11}$$

To ensure isotropy it is customary to specify the energy spectrum in terms of the total energy in all Fourier modes of the same length, via

$$\mathcal{E}_k=\zeta(|k|). \tag{12}$$

Choosing $\zeta(z)=l^2\zeta_0(lz)$, for appropriately normalized ζ_0, will give (6) (approximately), for every choice of l, as can be seen by comparison with an integral.

Noting that ζ_0 defines the shape of the spectrum $\{\lambda_k\}$, it follows that, given this shape, three parameters remain in the problem: τ, particle time constant/fluid time constant; $1/\nu$, nondimensional velocity correlation time; and l, nondimensional correlation length—where ζ peaks at $\mathcal{O}(1/l)$.

We have mentioned that the Stokes number plays a central role in the effect of preferential concentration. The Stokes number is defined as the ratio of the aerodynamic particle time constant to an *appropriate* turbulence time scale. One possible candidate for the Stokes number is therefore the parameter τ, with a fluid time constant based on the root mean square fluid velocity and length scale L. The parameter l sets the length scale of the coherent structures in the velocity field v while ν indicates how fast coherent structures decay, and new ones are born. In this paper we refer to τ as *the time scale ratio*, ν^{-1} *as the correlation time* and l *as the correlation length*. Note that definitions of a Stokes number other than τ can be obtained by combining values of the three parameters τ, l, and ν. In this paper we will *not* study the effect of varying the correlation length l, and it will be fixed at order one. However, the limit $l\to 0$ is of interest, and we will study it in future work.

We study two different spectra in our numerical experiments: the *Kraichnan* spectrum,[15]

$$\zeta_0(z)\propto z^2e^{-z^2},$$

and the *Kármán–Obukhov* spectrum,[19]

$$\zeta_0(z)\propto z^2(1+z^2)^{(-7/3)}.$$

Both produce similar results. For this paper all the numerical illustrations are performed using the second choice. There are some mathematical issues concerning the lack of regularity of the velocity field resulting from the second choice, but numerical experiments indicate that these are not manifest in the quantities we measure here.[32]

III. SCALING LIMITS

In this section we discuss the model (7) in various scaling limits of interest. In Sec. III A, we study the variation of the time scale ratio τ for fixed correlation time ν^{-1}; we elucidate the structure of the problem for $\tau\ll 1$ and $\tau\gg 1$. In Sec. III B we study variation with ν for fixed τ, elucidating the structure of the problem for $\nu\ll 1$ and $\nu\gg 1$. In Sec. III C we study various large-time scaling limits in which the velocity field is rapidly decorrelating, leading to Itô SDEs for the particle motion. Recall that, throughout, we fix the correlation length l at order one. We study the cases $\tau=O(1)$ and $\nu=O(1)$ numerically in Sec. IV.

A. Varying the time scale ratio

We study particle distributions according to the model (7) as τ, the time scale ratio, varies while ν^{-1}, the correlation time, and l, the correlation length, are fixed. We first summarize known properties in the limits $\tau=0,\infty$ in order to set the numerical experiments in context. For $\tau=0$ we obtain the model for particle tracers:

$$\dot{x}=v(x,t),$$

with v a Gaussian random field in space–time. These models do not exhibit preferential concentration. This can be seen as follows. Since particles follow incompressible fluid trajectories, passing to a continuum limit for a density $\rho(x,t)$ of particles located at position x at time t, we obtain the Liouville equation,

$$\frac{\partial\rho}{\partial t}+v\cdot\nabla\rho=0.$$

If $\rho(x,0)$ is uniform then $\rho(x,t)$ is uniform for all time, preventing preferential concentration.

For $\tau=\infty$ we obtain the equation for particles in a vacuum,

$$\ddot{x}=0.$$

Again, a Liouville argument, now for a density $\rho(x,\dot{x},t)$, shows that uniform particle distributions in position space x are preserved in time, provided that the initial velocities $\dot{x}$ are independent of the initial positions, and preferential concentration is ruled out.

In Sec. IV, we present numerical evidence to show that these conclusions about $\tau=0,\infty$ give an accurate picture of what happens for $\tau\ll 1$ and $\tau\gg 1$, at intermediate time scales. For τ of order one, however, we will demonstrate numerically that preferential concentration is observed. These findings are in agreement with experimental evidence, and evidence based on DNS, that preferential concentration occurs if and only if the Stokes number is of order one.[1]

B. Varying the fluid correlation time

We discuss how the model (7) behaves as ν^{-1}, the fluid correlation time, varies while τ, the time scale ratio, and l, the correlation length, is fixed. For $\nu=0$ (infinite correlation time) the velocity field is frozen and the equation of motion is

$$\tau\ddot{x}=v(x)-\dot{x},$$

with v a homogeneous, isotropic Gaussian random field in space. This equation is dissipative with a global attractor; physically this means that, asymptotically for large times, the particle velocities are bounded independently of their starting values. In fact, they are bounded asymptotically by the peak

fluid velocity. Over a short time, preferential concentration is not observed, but on a longer time interval the large time dynamics typically lead to preferential concentration. Numerical experiments indicate that for almost all initial conditions the solution converges to one of a finite number of isolated periodic orbits and then preferential concentration occurs. This limit is mathematically interesting, but far from any regimes observed in the experiments reviewed in Eaton and Fessler.[1] We do not pursue it further here.

To understand the limit $\nu\to\infty$, when the fluid decorrelates rapidly, we make a digression into the properties of OU processes. Let η solve

$$\frac{d\eta}{dt}+\alpha\nu\eta=\sqrt{\lambda\nu}\frac{d\beta}{dt}, \tag{13}$$

with β a standard Brownian motion and with stationary initial data. Then

$$\eta(t)=\sqrt{\lambda\nu}\int_{-\infty}^{t}e^{-\alpha\nu(t-s)}d\beta(s).$$

This is a Gaussian process with mean 0 and covariance,

$$\mathbb{E}\eta(t+T)\,\eta(t)=\frac{\lambda}{2\alpha}e^{-\alpha\nu T}.$$

For $\nu\gg 1$, we have

$$e^{-\alpha\nu t}\approx\frac{2\delta(t)}{\alpha\nu},$$

implying that $\eta(t)$ is approximately a white noise:

$$\eta(t)\approx\sqrt{\lambda/\nu\alpha^2}\frac{d\beta}{dt}. \tag{14}$$

Although this calculation is simply a heuristic, it is possible to make it precise by considering the solutions of equations driven by η solving (13), in the limit $\nu\to\infty$. Theorems can be proved in the sense of weak[33] and strong convergence[34] in various contexts. None of these results apply directly to our situation because of the particular infinite-dimensional form of our OU processes. Therefore we limit ourselves to a derivation of the limit equations, following the methodology in Majda *et al.*[4] and Kramer and Majda.[5] We leave the question of making the derivation rigorous for future study.

Using (13), (14) in (10), (9) we see that

$$v(x,t)\approx\frac{1}{\sqrt{\nu}}\sum_{k\in K}\nabla^{\perp}e^{ik.x}\frac{\sqrt{\lambda_k}}{\alpha_k}\frac{d\beta_k}{dt}:=\frac{1}{\sqrt{\nu}}\sigma(x)\frac{dB}{dt}. \tag{15}$$

Here $B=\{\beta_k\}_{k\in K}$ is an infinite-dimensional Brownian motion, and $\sigma(x)$: $\mathbb{C}^K\to\mathbb{C}^2$ is defined by

$$\sigma(x)\gamma=\sum_{k\in K}\nabla^{\perp}e^{ik\cdot x}\frac{\sqrt{\lambda_k}}{\alpha_k}\gamma_k,$$

for $\gamma=\{\gamma_k\}_{k\in K}\in\mathbb{C}^K$. Whenever one has a continuous approximation to white noise, the Stratonovich limit is to be expected. For the second-order dynamics (7), the noise in (15) may be interpreted in the Itô sense as the Itô and Stratonovich formulations do not differ because the diffusion coefficient depends only on particle position, not particle velocity. However, in the case of first-order dynamics (1), a more complicated argument also shows that the Itô and Stratonovich integrals are the same. This is because

$$\begin{aligned}\sigma(x)\sigma(x)^*&=\sum_{k\in K}\frac{\lambda_k}{\alpha_k^2}\nabla^{\perp}e^{ik\cdot x}(\nabla^{\perp}e^{ik\cdot x})^*\\&=\sum_{k\in K}\frac{\lambda_k}{\alpha_k^2}\begin{pmatrix}k_2\\-k_1\end{pmatrix}(k_2\quad -k_1)\\&=\sum_{k\in K}\frac{\lambda_k}{\alpha_k^2}\begin{pmatrix}k_2^2&-k_1k_2\\-k_1k_2&k_1^2\end{pmatrix}\\&=\left(\sum_{k\in K}\frac{\lambda_k}{2\alpha_k^2}|k|^2\right)I,\end{aligned}$$

so $\sigma(x)\sigma(x)^*\propto I$ (which is the Kubo formula here). Hence the Stratonovich–Itô conversion term disappears after noting that σ is divergence-free. Substituting (15) into (7), we obtain the approximation

$$\tau\frac{d^2x}{dt^2}=\frac{1}{\sqrt{\nu}}\sigma(x)\frac{dB}{dt}-\frac{dx}{dt}. \tag{16}$$

Letting $\nu\to\infty$, we deduce that, for an infinitely rapidly decorrelating fluid, particle motion is governed by

$$\tau\ddot{x}=-\dot{x}. \tag{17}$$

Again, a Liouville equation argument shows that initially uniform particle distributions in position space will be preserved, provided the velocities are chosen independently of positions—preferential concentration does not occur. Physically the velocity field is decorrelating so quickly that particles are unable to correlate with the fluid. [Note that, by rescaling time to $\mathcal{O}(\nu)$, Eq. (14) gives a nonzero white noise approximation as $\nu\to\infty$. In the next section we show that this can lead to preferential concentration over long time intervals, for $\tau\gg 1$ and $\nu\gg 1$.]

The case $\nu=\mathcal{O}(1)$ is the same as $\tau=\mathcal{O}(1)$ discussed in the previous section: numerical evidence presented in Sec. IV shows that preferential concentration does occur in this regime.

C. Large time behavior and rapidly decorrelating velocity field

By looking to large time and under appropriate scalings of the correlation time ν^{-1} and the time scale ratio τ, we can derive SDEs for particle motion. We rescale time, the time scale ratio, and the correlation time by setting

$$t=s\gamma,\quad \tau=\tau_0\gamma^{\alpha},\quad \nu=\gamma^{\beta}.$$

Here $\gamma\gg 1$. Let v_0 denote a velocity field obtained from (7) with $\nu=1$.

Stokes' law then gives

$$\tau_0\frac{d^2x}{ds^2}=\gamma^{2-\alpha}v_0(x,\gamma^{1+\beta}s)-\gamma^{1-\alpha}\frac{dx}{ds}. \tag{18}$$

Alternatively, multiplying by $\gamma^{\alpha-1}$, we may write this as

$$\gamma^{\alpha-1}\tau_0\frac{d^2x}{ds^2}=\gamma v_0(x,\gamma^{1+\beta}s)-\frac{dx}{ds}. \tag{19}$$

Note that $v(x,t)$ appearing in (15) is given by $v_0(x,t\nu)$. Thus, (15) shows that, for $\epsilon\ll 1$,

$$v_0(x,t/\epsilon)\approx\sqrt{\epsilon}\sum_{k\in K}\nabla^{\perp}e^{ik.x}\frac{\sqrt{\lambda_k}}{\alpha_k}\frac{d\beta_k}{dt}:=\sqrt{\epsilon}\sigma(x)\frac{dB}{dt}. \tag{20}$$

In order to obtain a balance between the effect of the velocity field and the inertial terms, it is necessary to choose the amplitude of the rescaled velocity field to scale as the square root of the time dilation factor. Thus, to retain an interesting white noise effect in (18), we must choose $2(2-\alpha)=1+\beta$ so that $2\alpha+\beta=3$. To retain an interesting white noise effect in (19) we must choose $\beta=1$. Ensuring that white noise remains in the limit $\gamma\to\infty$, and that it balances at least one of the remaining terms, leads to the following three cases, describing the limit $\gamma\to\infty$. When interpreting the three cases note that $\alpha<0/\alpha>0$ corresponds to small/large time scale ratios, while $\beta<0/\beta>0$ corresponds to long/short fluid correlation times.

Case 1. $\alpha\in(-\infty,1)$, $\beta=1$: here inertial effects are negligible and we recover the passive tracer model,

$$\frac{dx}{ds}=\sigma(x)\frac{dB}{ds}. \tag{21}$$

Since $\sigma(x)\sigma(x)^*\propto I$ this predicts Brownian motion for the *position* of a single particle, and is a well-known limit (Ref. 25, Sec. 4.1). We do not expect preferential concentration in this limit because the velocity field $\sigma(x)dB/dt$ is still incompressible.

Case 2. $\alpha\in(1,2)$, $\beta=3-2\alpha\in(-1,1)$: here the large particle mass (more precisely the large time scale ratio) leads to a balance between the inertial terms and the fluid velocity, with particle drag being negligible. The resulting limit is the equation

$$\tau_0\frac{d^2x}{ds^2}=\sigma(x)\frac{dB}{ds}. \tag{22}$$

Since $\sigma(x)\sigma(x)^*\propto I$, this predicts Brownian motion for the *velocity* of a single particle. Preferential concentration cannot occur in this regime in situations where initial particle distributions are uniform in position and velocity space; numerical experiments are needed to determine what happens for initial data which are not of this form.

Case 3. $\alpha=\beta=1$: this case describes the large-time behavior of a heavy particle (more precisely, with a large time scale ratio) in a rapidly decorrelating fluid. This results in an equation where inertial effects balance viscous drag and forcing due to the fluid velocity, resulting in the equation

$$\tau_0\frac{d^2x}{ds^2}=\sigma(x)\frac{dB}{ds}-\frac{dx}{ds}. \tag{23}$$

Since $\sigma(x)\sigma(x)^*\propto I$, this predicts an Ornstein–Uhlenbeck process for the velocity of a single particle. Preferential concentration is possible in this regime and numerical results are presented in Sec. V. The physical mechanism for the preferential concentration observed in Case 3 is as follows. When viewed in position *and velocity* space simultaneously, the dynamics of (7) is compressible—volumes are contracted, forcing particles into tiny regions of velocity/position space after times of order τ. By looking at a scaling in which time is or order τ, and τ is assumed large, and the velocity decorrelates rapidly, these tiny regions in velocity/position space where particles gather exhibit fluctuations in time and encapsulate the preferential concentration.

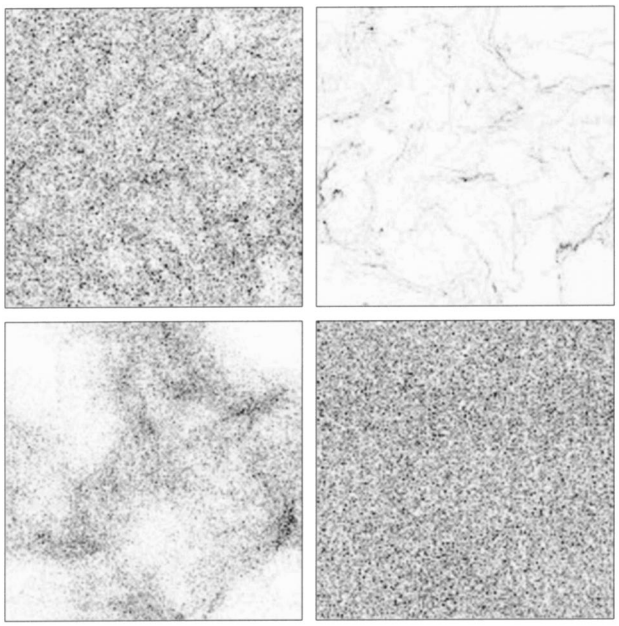

FIG. 3. Particle distributions for (7), without collisions, at $\nu=10^{-2}$, for $\tau=10^k$, $k=-2,-1,0,1$ (left to right, top to bottom).

Note that Case 1 follows from Eq. (19) while Case 2 follows from (18). Case 3 is the marginal case between these two. We do not allow $\alpha\geqslant 2$ because then $1+\beta\leqslant 0$ and the velocity field $v_0(x,\gamma^{1+\beta}s)$ is not rapidly decorrelating.

IV. EFFECT OF TIME SCALE RATIO: NUMERICS

In this section and the next we present results of numerical simulations of the model (7). Our numerical method is comprised of three parts: (i) an evolution of ψ and v in Fourier space, using the FFT to return to physical space; (ii) a linearly implicit evolution of the ODEs for particle motion; (iii) the use of a fast and accurate collision detection algorithm for particles in a time-evolving field.[29] The use of a random field model for the velocity field leads to an order of magnitude saving when compared with DNS based on the Navier–Stokes equation.

For our experiments we use the Kármán–Obukhov spectrum and fix the turbulence length scale l at order one. Thus, the two free parameters are the time scale ratio τ and the correlation time ν^{-1}. In addition, when collisions are calculated, the percentage of volume occupied by the particles, ρ, is relevant. Our experiments can be summarized as follows: we fix $\nu=10^{-2}$ and then (1) let τ vary from 10^{-2} to 10^1; (2) add collisions and, for $\tau=0.1$ and $\tau=1$, let the particle volume density ρ vary from 0.01% to 10%.

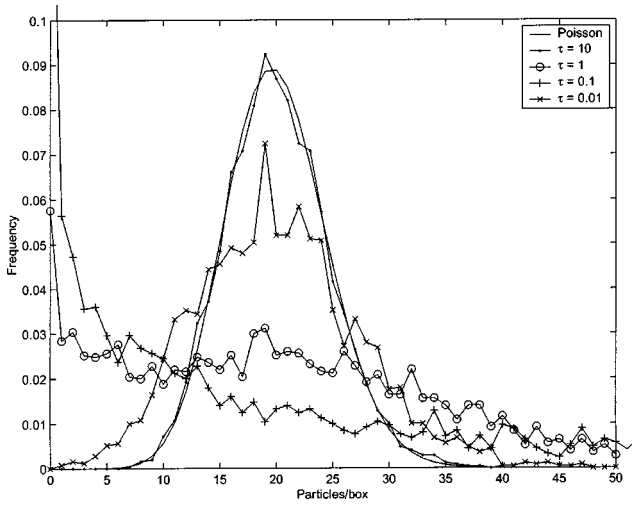

FIG. 4. Particle distributions for (7), without collisions, at $\nu=10^{-2}$.

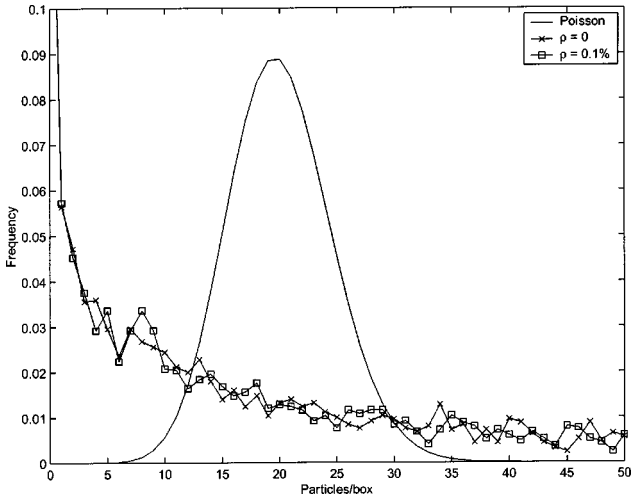

FIG. 6. Particle distributions for (7), with collisions, at $\nu=10^{-2}$ and $\tau=0.1$.

Figures 3–8 show the resulting particle distributions at $T=3$.

The main results of the simulations without collisions can be summarized as follows: *preferential concentration occurs when τ is of order one, but not at large or small values of τ.* This fact is evident from Fig. 3, in that the particle distribution is nonuniform at $\tau=0.1$ and $\tau=1$, but spatially homogeneous for $\tau=0.01$ and $\tau=10.0$. This is quantified in Fig. 4, which compares particle distributions with the Poisson case; only $\tau=0.1$ and $\tau=1$ show significant departure from Poisson behavior. Comparing Fig. 4 to the real experimental data in Fig. 2, we see that at the intermediate "Stokes number," $\tau=1$, even the *quantitative* agreement with experiment is remarkably good.

Now to the addition of collisions. Again we can summarize the results in a single sentence: *elastic collisions do not greatly affect particle distributions at low densities*. This is evident from Figs. 5 and 7; the effect of collisions is hardly noticeable until $\rho=10\%$. Figures 6 and 8 also clearly show that adding collisions does not change the quantitative comparison with Fig. 2 significantly.

The only noticeable effect of collisions at low densities is, however, quite interesting. Note from Fig. 3 that preferential concentration is more pronounced at $\tau=0.1$ than $\tau=1$ in that the particles concentrate more tightly for $\tau=0.1$. One might therefore expect that the effect of collisions would be greater at $\tau=0.1$ than at $\tau=1$. Surprisingly, the opposite is true, as Figs. 5 and 7 indicate. The observation can probably be explained by the variation in particle velocity field in space and time, variation that is probably greater at $\tau=1$ than at $\tau=0.1$; we have not verified this, however, as

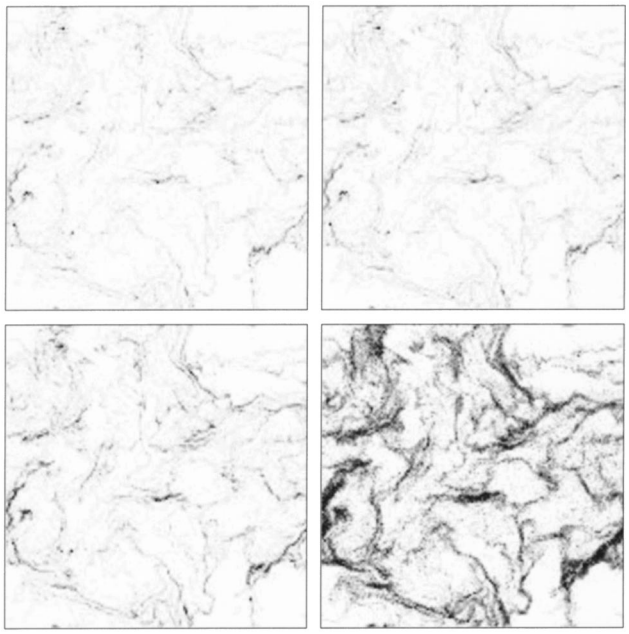

FIG. 5. Particle distributions, for (7), with collisions, at $\nu=10^{-2}$ and $\tau=0.1$, for $\rho=0\%$, 0.1%, 1%, and 10% (left to right, top to bottom).

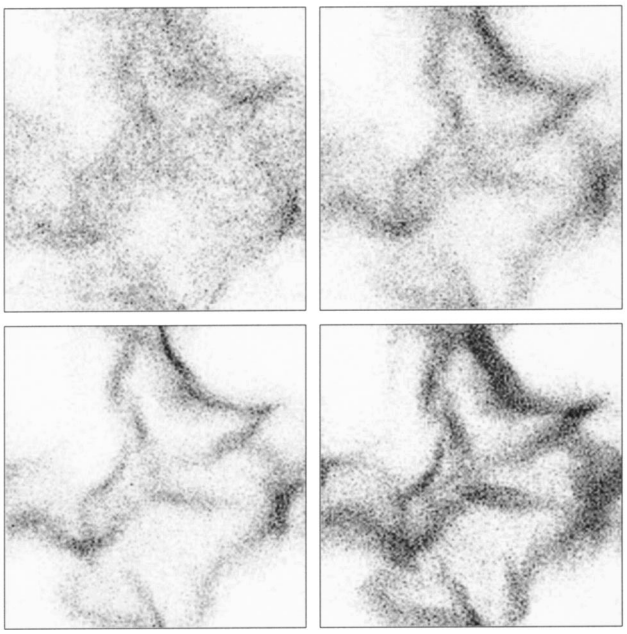

FIG. 7. Particle distributions for (7), with collisions, at $\nu=10^{-2}$ and $\tau=1$, for $\rho=0\%$, 0.1%, 1%, and 10% (left to right, top to bottom).

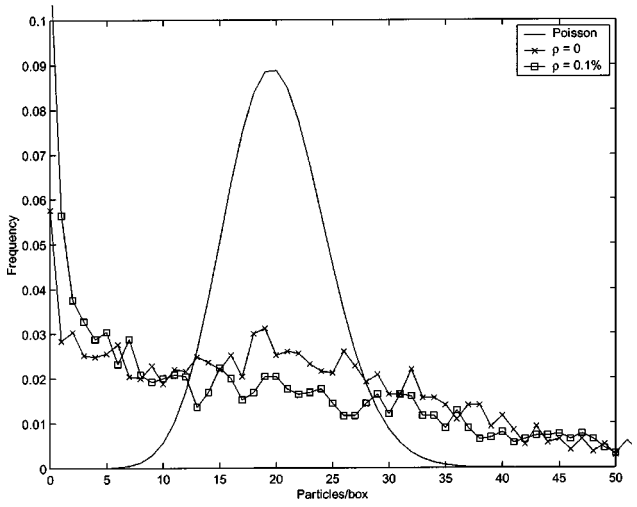

FIG. 8. Particle distributions for (7), with collisions, at $\nu=10^{-2}$ and $\tau=1$.

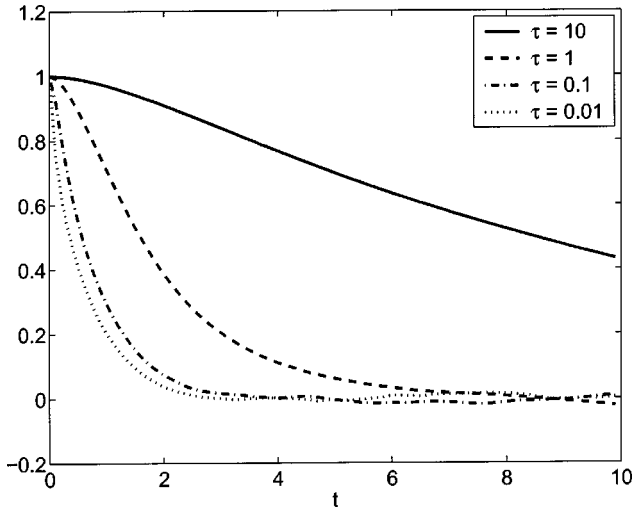

FIG. 10. Autocorrelation function of a single velocity component for a particle obeying (7), for different τ.

it requires substantial work. This observation is further quantified in Figs. 6 and 8. In particular, Fig. 8 shows an antidiffusive effect introduced by collisions: collisions enhance the sharp concentration lines in particle distributions.

We also run the algorithm tracking the motion of a single particle. We use the same setup as before with $\nu=10^{-2}$ and vary τ from 10^{-2} to 10. Some results are shown in Figs. 9 and 10. The velocity distribution is Gaussian; the depicted distribution is of the x_1 component of the velocity at $\tau=0.1$, and other values of τ give indistinguishable results. Also, long-range correlations exist at large τ since then the particle is not greatly affected by the velocity field. At small τ the correlations are only short lived, but remain finite as $\tau\to 0$; the remaining correlations are inherited from the velocity field.

V. RAPIDLY DECORRELATING VELOCITY FIELD: NUMERICS

Our aim in this section is to study Eq. (23), governing the large time behavior of the particle position x when τ and ν are large, by means of numerical experiments. Recall that for τ and/or ν large preferential concentration is not expected at order one times. First note that, once again, particle velocity distributions are approximately Gaussian—see Fig. 11. For small τ_0, we expect to see a delta-like velocity autocorrelation, as x is then approximately Brownian motion [recall that $\sigma(x)\sigma(x)^*\propto I$]. This is indeed the case—Fig. 12 shows the autocorrelation for different τ_0, clearly showing convergence to a scaled delta function as $\tau_0\to 0$.

The numerical experiments are similar to those in the previous section, but in the rapidly decorrelating limit of large ν. We integrate the white noise approximation (23) to time $s=10^4$. Figure 13 shows particle distributions at this

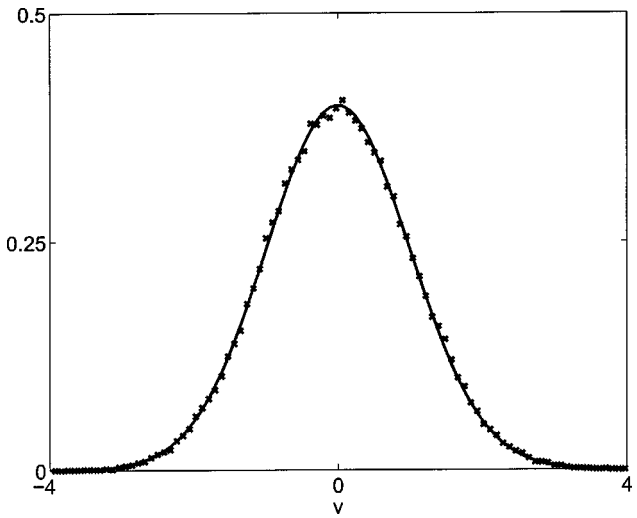

FIG. 9. Typical distribution of a velocity component of x, from the time series of a single particle obeying (7), compared with the Gaussian distribution.

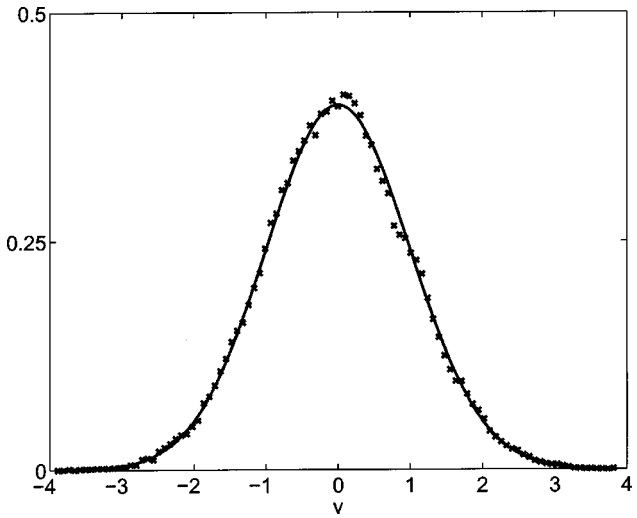

FIG. 11. Typical distribution of a velocity component of x, from the time series of a single particle obeying (23), compared with the Gaussian distribution.

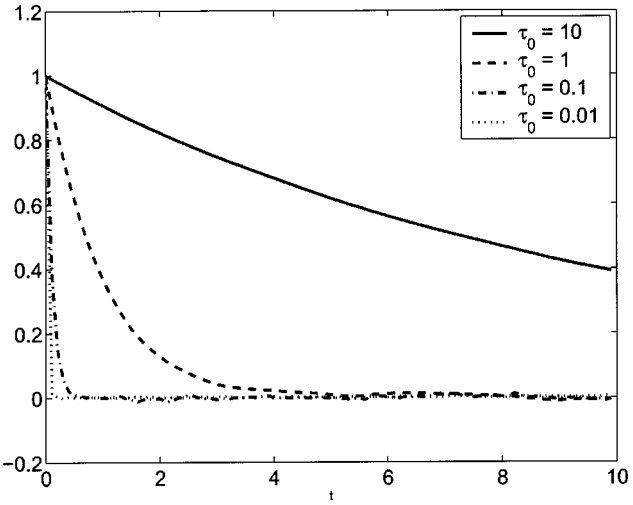

FIG. 12. Autocorrelation function of a single velocity component for a particle obeying (23), for different τ_0.

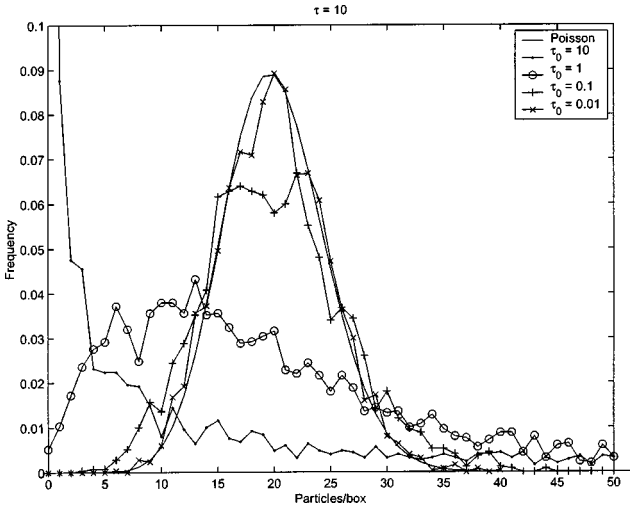

FIG. 14. Particle distributions for (23), without collisions, in the white noise limit at $\nu=1$ for different τ_0.

time, for varying τ_0, and Fig. 14 shows the particles-per-box histogram from the same data. It is clear that preferential concentration is indeed observed for a range of τ_0.

Thus, the model (7) predicts that, over long time intervals, inertial particles can correlate with one another, even when placed in a rapidly decorrelating vector field. It would be of interest to determine whether this prediction is borne out in real experiments and/or simulations using DNS of the Navier–Stokes equations, or whether it is caused by the simplistic nature of the Gaussian random field model for the velocity.

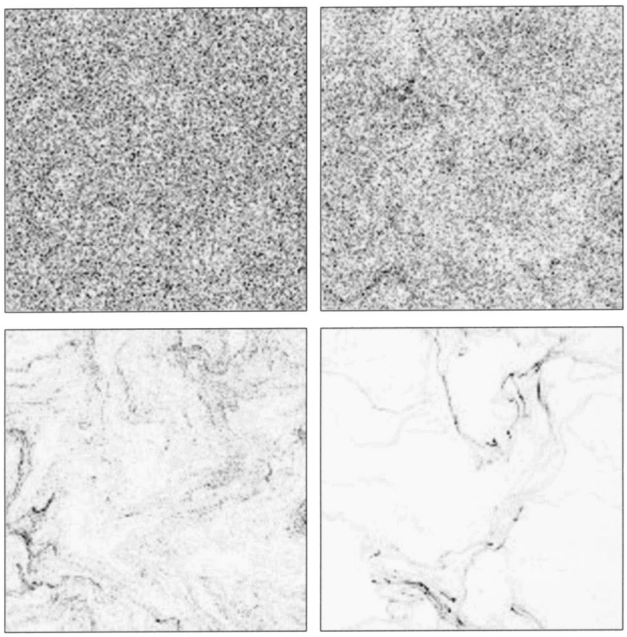

FIG. 13. Particle distributions for (23), without collisions, in the white noise limit at $\nu=1$ for $\tau_0=10^k$, $k=-2,-1,0,1$ (left to right, top to bottom).

VI. CONCLUSIONS

In this paper we have presented a simple model for the motion of inertial particles in a turbulent fluid. The model comprises Stokes' law for the particle motion, with fluid velocity modeled by a Gaussian random field. The model is very fast to simulate from, including the effect of collisions, and is also amenable to mathematical analysis. Its primary limitations stem from the limited validity of Stokes' law, when the fluid and particle velocities differ substantially, and from the inability of the Gaussian random field model of a turbulent fluid to capture energy transfer between scales. Although our work is in two dimensions, it would be possible to generalize the approach to three dimensions by working with a pair of independent linear stochastic PDEs whose solutions at wave vector k span the 2-D orthogonal complement of k, leading to a divergence-free velocity field with a prescribed spectrum.

Despite the limitations of the model, it compares well with real experimental data in the sense that, for a time scale ratio of order one, particle distributions differ substantially from Poisson behavior. It would be of interest to make more detailed comparisons between the model and the wealth of experimental data and data based on DNS for the fluid.

Using the simple model we have investigated numerically the effect of collisions on preferential concentration, showing that it is negligible for the low densities at which our model is valid; however, an interesting antidiffusive effect is observed at moderate particle densities. The model also allows the derivation of stochastic differential equations governing particle distributions over large times; in particular, when time, the particle/fluid time scale ratio, and the inverse correlation time of the fluid are all large, then the stochastic model again predicts preferential concentration. A further comparison with DNS will be required to determine whether this prediction of the model reflects a real physical phenomenon, or whether it reflects the simple statistical model used for the fluid velocity. Assuming that the predictions are valid, it is noteworthy that the model used here then

provides a substantial advantage over DNS models because the scaling analysis leading to stochastic differential equations facilitates the probing of parameter regimes that are not amenable to DNS.

ACKNOWLEDGMENTS

The authors are grateful to A. J. Majda for helpful suggestions. H.S. was supported by the Department of Energy under the ASCI, Program. A.M.S. was supported by the Engineering and Physical Sciences Research Council of the UK.

[1]J. K. Eaton and J. R. Fessler, ''Preferential concentration of particles by turbulence,'' Int. J. Multiphase Flow **20**, 169 (1994).
[2]K. D. Squires and J. K. Eaton, ''Particle response and turbulence modification in isotropic turbulence,'' Phys. Fluids A **2**, 1191 (1990).
[3]J. R. Fessler, J. D. Kulick, and J. K. Eaton, ''Preferential concentration of heavy particles in a turbulent channel flow,'' Phys. Fluids **6**, 3742 (1994).
[4]A. J. Majda, I. Timofeyev, and E. Vanden Eijnden, ''A mathematical framework for stochastic climate models,'' Commun. Pure Appl. Math. **54**, 891 (2001).
[5]P. Kramer and A. J. Majda, ''Stochastic mode elimination applied to simulation methods for complex microfluid systems,'' SIAM J. Appl. Math. (in press).
[6]K. D. Squires and J. K. Eaton, ''Measurements of particle dispersion obtained from direct numerical simulations of isotropic turbulence,'' J. Fluid Mech. **226**, 1 (1991).
[7]K. D. Squires and J. K. Eaton, ''Preferential concentration of particles by turbulence,'' Phys. Fluids A **3**, 1169 (1991).
[8]R. C. Hogan, J. N. Cuzzi, and A. R. Dobrovolskis, ''Scaling properties of particle density fields formed in simulated turbulent flows,'' Phys. Rev. E **60**, 1674 (1999).
[9]T. Elperin, N. Kleeorin, and I. Rogachevskii, ''Self-excitation of fluctuations of inertial particle concentration in turbulent fluid flow,'' Phys. Rev. Lett. **77**, 5373 (1996).
[10]T. Elperin, N. Kleeorin, and I. Rogachevskii, ''Dynamics of particles advected by fast rotating turbulent fluid flow: Fluctuations and large scale structures,'' Phys. Rev. Lett. **81**, 2898 (1998).
[11]A. Crisanti, M. Falcioni, A. Provenzale, and A. Vulpiani, ''Passive advection of particles denser than the surrounding fluid,'' Phys. Lett. A **150**, 79 (1990).
[12]S. Sundaram and L. R. Collins, ''Collision statistics in an isotropic particle-laden turbulent suspension. Part 1. Direct numerical simulations,'' J. Fluid Mech. **335**, 75 (1997).
[13]A. Bracco, P. H. Chavanis, A. Provenzale, and E. A. Spiegel, ''Particle aggregation in a turbulent Keplerian flow,'' Phys. Fluids **11**, 2280 (1999).
[14]M. R. Maxey, ''Gravitational settling of aerosol particles in homogeneous turbulence and random flow fields,'' J. Fluid Mech. **174**, 441 (1987).
[15]R. H. Kraichnan, ''Diffusion by a random velocity field,'' Phys. Fluids **13**, 22 (1970).
[16]A. Careta, F. Sagueés, and J. M. Sancho, ''Stochastic generation of homogeneous isotropic turbulence with well-defined spectra,'' Phys. Rev. E **48**, 2279 (1993).
[17]A. C. Martí, J. M. Sancho, F. Sagués, and A. Careta, ''Langevin approach to generate synthetic turbulent flows,'' Phys. Fluids **9**, 1078 (1997).
[18]A. Juneja, D. P. Lathrop, K. R. Sreenivasan, and G. Stolovitzky, ''Synthetic turbulence,'' Phys. Rev. E **49**, 5179 (1994).
[19]J. García-Ojalvo and J. M. Sancho, *Noise in Spatially Extended Systems* (Springer-Verlag, New York, 1999).
[20]G. I. Taylor, ''Diffusion by continuous movements,'' Proc. London Math. Soc. **20**, 196 (1921).
[21]A. Fannjiang and T. Komorowski, ''Diffusions in long-range correlated Ornstein–Uhlenbeck flows,'' Elect. J. Prob. 7, 1 (2002).
[22]T. Komorowski and G. Papanicolaou, ''Motion in a Gaussian, incompressible flow,'' Ann. Prob. **7**, 229 (1997).
[23]R. Carmona and L. Xu, ''Homogenization for time dependent 2D incompressible Gaussian flows,'' Ann. Appl. Probab. **7**, 265 (1997).
[24]R. Carmona, S. Grishin, S. A. Molchanov, and L. Xu, ''Surface stretching for Ornstein Uhlenbeck velocity fields,'' Electron. Comm. Probab. **2**, 1 (1997).
[25]A. J. Majda and P. R. Kramer, ''Simplified models for turbulent diffusion: Theory, numerical modeling, and physical phenomena,'' Phys. Rep. **314**, 237 (1999).
[26]H. Kunita, *Stochastic Flows and Stochastic Differential Equations* (Wiley, New York, 1978).
[27]A. Fannjiang, L. Ryzhik, and G. Papanicolaou, ''Evolution of trajectory correlations in steady random flows,'' Proc. Symp. Appl. Math. **54**, 105 (1998).
[28]H. Kesten and G. Papanicolaou, ''A limit theorem in turbulent diffusion.'' Commun. Math. Phys. **65**, 97 (1979).
[29]H. Sigurgeirsson, A. M. Stuart, and W.-L. Wan, ''Algorithms for particle-field simulations with collisions,'' J. Comput. Phys. **172**, 766 (2001).
[30]G. K. Batchelor, *An Introduction to Fluid Dynamics* (Cambridge University Press, Cambridge, 1967).
[31]R. Clift, J. R. Grace, and M. E. Weber, *Bubbles, Drops, and Particles* (Academic, New York, 1978).
[32]H. Sigurgeirsson and A. M. Stuart, ''Inertial particles in a random field,'' Stochastics Dyn. **2**, 295 (2002).
[33]T. Kurtz, ''A limit theorem for perturbed operator semigroups with applications to random evolutions,'' J. Funct. Anal. **12**, 55 (1973).
[34]R. M. Dowell, ''Differentiable approximation to Brownian motion on manifolds,'' Ph.D. thesis, University of Warwick, 1980.